The evaluation of endothelial cell migration for proper endothelialization in artificial blood vessels

Jae Kyeong Kang

Department of Medical Science
The Graduate School, Yonsei University

The evaluation of endothelial cell migration for proper endothelialization in artificial blood vessels

Directed by Professor Jong-Chul Park

The Master's Thesis
submitted to the Department of Medical Science,
the Graduate School of Yonsei University
in partial fulfillment of the requirements for the
degree of Master of Medical Science

Jae Kyeong Kang

June 2010

This certifies that the Master'sThesis of Jae Kyeong Kang is approved.

Thesis Supervisor : Jong-Chul Park

Ji Hoe Heo

Soo Hyun Kim

The Graduate School
Yonsei University

June 2010

ACKNOWLEDGEMENTS

지난 2년은 생각보다 빠르게 지나간 것 같습니다. 실험을 할 때 지금 내가 잘 하고 있는 건지 아닌 건지 조급해 했었던 것 같은 데 그럴 때마다 많은 말씀 해주시고 올바른 방향으로 이끌어 주신 박종철 교수님께 진심으로 감사드립니다. 교수님의 충고와 따뜻한 가르침 덕분에 끝까지 마무리를 잘 지을 수 있었습니다. 또한 논문이 완성되기 까지 친히 시간을 내어 도움을 주신 허지회 교수님, 김수현 교수님께도 지면을 빌어 감사의 말씀드립니다.

2년을 아무 탈 없이 잘 지낼 수 있었던 가장 큰 이유는 서로를 배려해주는 실험실 분위기 덕분이었던 것 같습니다. 실험할 때 문제 해결에 있어서 다양한 아이디어를 제공해주셨던 박봉주 박사님과 한인호 박사님, 조금 더 이야기를 많이 나눠보았으면 하는 아쉬움이 남는 김학희 박사님, 어려운 일을 헤아려 준 고마운 현숙언니, 예쁜 아가 엄마가 된 혜련언니, 말도 안 되는 장난 다 받아준 대형오빠, 엄마 같이 챙겨주는 미희언니, 언니가 만든 푸딩이 제일 맛있어요 혜리언니, 이젠 그냥 한국 친구 같은 내 유일한 동기 Barbora, 동생이 맞는지 헷갈리는 병주, 아침밥 동지 정현이, 엉뚱한 막둥이 여송이, 한국에 있는 것만 같은 연이언니, 돈 버느라 고생하는 수창오빠, 독일에서 열심히 공부하고 있을 동정언니, 지금쯤 힘들텐데 열심히 공부하고 있을 민성이까지 다들 고맙습니다. 덕분에 실험실 생활이 너무 즐거웠고 잊을 수 없는 추억 한가득 안고 갑니다.

호주에서 어려움 겪을 때 옆에서 챙겨주었던 너무나도 고마운 한동욱 박사님, 현용오빠, 종호, 선배로써 많이 챙겨주지 못해 미안한 주현이와 소혜, 언제나 내 편이고 어디서나 빛이 나는 슈퍼우먼들인 미라, 보람, 우리, 윤주, 지민, 지연, 지영, 그리고 정말 다 잘 될 것이

라고 말해주고 싶은 내겐 비타민 같은 존재들 경현, 설화, 성진, 민정, 생각만으로도 20살이 너무 그립게 만드는 민희, 성미, 유정, 주희, 그리고 아직도 공학1반이라는 이름으로 만나는 강아지들, 우리 만난 지 16년이 됐다고 믿겨지지 않는 완전한 인연 혜진, 희진, 민진, 어느 순간 정말 편한 동네 친구들이 된 은경, 명은, 준영, 명호, 성민, 모두들 너라면 잘 할 수 있다라고 격려해주고 아직 학생이라며 배려해주던 예쁜 마음들 잊지 않겠습니다.

마지막으로 저에겐 항상 최고인 가족들 감사합니다. 누구보다 저의 결정을 지지해주시고 믿어주시는 부모님과 오히려 누나를 챙겨주는 믿음직스러운 동생 동보, 말로 표현할 수 없을 만큼 사랑합니다. 아버지, 어머니의 관심과 후원 덕분으로 제가 이만큼 성장할 수 있었습니다. 앞으로 기대에 어긋나지 않는 딸로 보답하겠습니다.

비록 석사 과정은 끝났지만 또다른 새로운 시작에 앞서 많은 분들을 염려시키지 않도록 늘 노력하는 사람이 되겠습니다.

2010년 6월

강 재 경 드림

Table of contents

Abstract ····· 1
I. INTRODUCTION ····· 3
1. Endothelial cell migration ····· 3
2. Artificial blood vessel ····· 4
3. Mechanotaxis ····· 5
4. Scaffold for tissue engineering ····· 7
5. Objectives of this study ····· 8
II. MATERIALS AND METHOD ····· 9
1. Cells and cell cultures ····· 9
2. Cell seeding models ····· 9
3. Parallel plate chamber system ····· 10
4. Immunostaining ····· 13
5. Time-lapse phase contrast microscopy and Analysis of cell migration. ····· 14
A. Image acquisition ····· 14
B. Cell tracking and evaluation of cell migration ····· 14
6. HUVECs migration into scaffold in response of flow ····· 17
A. PLLA scaffold ····· 17
B. Cell seeding of scaffold ····· 17
C. The flow perfusion system ····· 18
D. Observation of cells distribution in scaffold ····· 18
7. Statistical analysis ····· 21

III. RESULTS ····· 22
1. Movement of HUVECs in accordance with the shear stress in wound closure model. ····· 22
2. Directional migration of HUVECs in wound closure model. ····· 24
3. Movement of HUVECs in accordance with the shear stress in individual cell migration model. ····· 26
4. Directional migration of HUVECs in individual cell migration model. ····· 28
5. Laminar flow VS Pulsatile flow ····· 30
6. Focal adhesion formation and actin cytoskeleton alignment ····· 32
7. HUVECs migration into scaffold in response of flow ····· 36
IV. DISCUSSION ····· 39
V. CONCLUSION ····· 43
REFERENCES ····· 44
ABSTRACT (IN KOREAN) ····· 49

Figure legends

Figure 1. Arterial wall showing endothelial cell and blood flow ··· 06

Figure 2. Schematic diagram of the parallel-plate flow chambers in a flow system for the evaluation of the cell migration. ····· 12

Figure 3. The evaluation of cell migration (A) Schematic of accumulated distance and Euclidean distance of cell movements. (B) X forward migration index (X_{FMI}) ····· 16

Figure 4. HUVECs migration into scaffold in response of flow. (A) Schematic diagram of the flow perfusion system for the evaluation of the cell migration into the scaffold. (B) Microfibrous PLLA scaffold. Microfibrous scaffolds which weigh 80 mg were prepared (left) and each of these was placed in a separate well of a 24 well tissue-culture plate for cell seeding (right). ····· 20

Figure 5. Movement of HUVECs in accordance with the shear stress in wound closure model. (A) The migration speed of HUVECs. (B) The directionality of HUVECs. Analyzed by Mann-Whitney U test and statistical significance was considered as $p < 0.0167$. These results were derived from measurements on 10 cells both upstream and downstream edge from 3 separate experiments. Values were means ±SE. The results are shown as a mean standard deviation (n = 30). * $p < 0.0167$ compared with static condition (0

dyne/cm^2), # $p < 0.0167$ compared with upstresam part. ‥ ····· 23

Figure 6. Directional migration of HUVECs in wound closure model. Analyzed by Mann-Whitney U test and statistical significance was considered as $p < 0.0167$. These results were derived from measurements on 10 cells from 3 separate experiments. Values were means ±SE. The results are shown as a mean standard deviation (n = 30). * $p <$ 0.0167 compared with static condition (0 dyne/cm^2) ····· 25

Figure 7. Movement of HUVECs in accordance with the shear stress in individual cell migration model. (A) The migration speed of HUVECs. (B) The directionality of HUVECs. Analyzed by Mann-Whitney U test and statistical significance was considered as $p < 0.0167$. These results were derived from measurements on 10 cells from 3 separate experiments. Values were means ±SE. The results are shown as a mean standard deviation (n = 30). * $p <$ 0.0167 compared with static condition (0 dyne/cm^2), # $p <$ 0.0167 compared with 4 dyne/cm^2. ····· 27

Figure 8. The directional migration of HUVECs in individual cell migration model. (A) X_{FMI} of HUVECs. Analyzed by Mann-Whitney U test and statistical significance was considered as $p < 0.0167$. These results were derived from measurements on 10 cells from 3 separate experiments.

Values were means ±SE. The results are shown as a mean standard deviation (n = 30). * $p < 0.0167$ compared with static condition (0 dyne/cm^2), # $p < 0.0167$ compared with 4 dyne/cm^2. (B) Trajectories of HUVECs. During 7 hours all cells were assumed to originate at (0,0) under static conditions and fluid shear stress (4 dyne/cm^2, 8 dyne/cm^2). The movement of 20 cells is shown. ····· 29

Figure 9. Comparision with cell migration under pulastile flow and laminar flow. (A) Cell migration speed (B) Directionality (C) X_{FMI}. All experiments were carried out at 8 dyne/cm^2 for 7 hours. Analyzed by Mann - Whitney U test and statistical significance was considered as $p < 0.0167$. These results were derived from measurements on 10 cells from 3 separate experiments. Values were means ±SE. The results are shown as a mean standard deviation (n = 30). * $p < 0.0167$ compared with static condition (0 dyne/cm^2), # $p < 0.0167$ compared with pulsatile flow. ····· 31

Figure 10. Immunostaining of vinculin, actin cytoskeleton and nucleus under static condition (A) Vinculin was stained with Texas Red conjugated antibody (red) and (B) Actin cytoskeleton was stained with Alexa (488)-conjugated phalloidin (green) and (C) Nucleus was stained with Hoechst #33258 (blue) and (D) merged imaged were

shown. Scale bar = 50um ····· 33

Figure 11. Immunostaining of vinculin, actin cytoskeleton and nucleus under flow condition. Shear stress was applied for 5 hours (A) Vinculin was stained with Texas Red conjugated antibody (red) and (B) Actin cytoskeleton was stained with Alexa (488) - conjugated phalloidin (green) and (C) Nucleus was stained with Hoechst #33258 (blue) and (D) merged imaged were shown. Scale bar = 50um ····· 34

Figure 12. Immunostaining of vinculin, actin cytoskeleton and nucleus under flow condition. Shear stress was applied for 30 minuts (A) Vinculin was stained with Texas Red conjugated antibody (red) and (B) Actin cytoskeleton was stained with Alexa (488)-conjugated phalloidin (green) and (C) Nucleus was stained with Hoechst #33258 (blue) and (D) merged imaged were shown. Scale bar = 50 um 35

Figure 13. Cross sectional area of confocal image for cell invasion into Scaffold. (A) under static condition for 12 hr. (B) under static condition for 24 hr. (C) Under flow condition for 12 hr (D) Under flow condition for 24hr. Scare bar = 100 um ····· 37

Figure 14. The invasion depth of HUVECs into scaffold in response of flow. Cells penetrated into scaffolds more than the static condition under flow condition. ····· 38

Abbreviations

ECs : Vascular endothelial cells

ECM : Extracellular matrix

ePTFE : Polytetrafluoroethylene

FBS : Fetal bovine serum

PBS : Phosphate buffered saline

CCD : Charge-coupled device

3D : Three dimensional

HUVECs : Human umbilical endothelial cells

EBM-2 : Endothelial basal medium-2

BSA : Bovine serum albumin

CCP : Composition controlling program

MC : Dichloromethane

FMI : Forward migration index

FAs : Focal adhesions

FAK : Focal adhesion kinase

Abstract

The evaluation of endothelial cell migration for proper endothelialization in artificial blood vessels

Jae Kyeong Kang

Department of Medical Science

The Graduate School, Yonsei University

(Directed by Professor Jong-Chul Park)

The main reason of restenosis that happened after bypass surgery, balloon angioplasty or stent placement is the damage of the endothelium, which generally forms the inner lining of the blood vessel walls. A rapid reendothelialization of the blood vessel walls is crucial for the prevention of thrombosis and intimal hyperplasia. Endothelial cell migration is critical and initiating the repair of injured vessels. Most of the researches on EC migration were completed under static conditions, but endothelial cells *in vivo* are under flow condition. Shear stress can induce many changes in endothelial cells, including alterations in cell shape, orientation, proliferation, and the reorganization of cytoskeleton etc.

In this study, we set up the parallel plate chamber system to evaluate endothelial cell migration under flow condition. In wound closure model, the cells in the upstream part more migrated into the wound area under flow condition compared with in the absence of flow, while shear stress

inhibited cell migration in the direction to the wound area in downstream part. In individual cell migration model, human umbilical endothelial cells started to migrate in the direction of flow at 8 dyne/cm^2. We observed focal adhesions formation at the leading edge of the cell in the direction of flow and the alignment of actin cytoskeleton at 8 dyne/cm^2. Also the flow perfusion system was estabilished for the effective cell seeding into a three dimensional scaffold. In this study, we found that under flow condition a better and more uniform cell distribution throughout the matrix was achieved than under static condition.

This study has demonstrated the possiblity to evaluate and analyze cell migration using the parallel plate chamber system and we may predict *in vivo* cell migration under flow condition based on these results. It may give some help to design stent or artificial blood vessels.

Key Words : Vascular Endothelial cell, cell migration, fluid shear stress, parallel plate chamber, mechanotaxis, scaffold

The evaluation of endothelial cell migration for proper endothelialization in artificial blood vessels

Jae Kyeong Kang

Department of Medical Science
The Graduate School, Yonsei University

(Directed by Professor Jong-Chul Park)

I. Introduction

1. Endothelial Cell migration

Vascular endothelial cells (ECs) form a monolayer lining the inside surface of blood vessel walls and play important roles in physiology of blood vessel walls.[1] For example, endothelial cells have a large variety of physiologically significant roles in regulation of permeability between blood and surrounding tissues, coagulation of blood, transmigration of leukocytes and regulation of vessel diameter.[1] The damage of vascular endothelium can occur for many reasons such as angioplasty and bypass procedures. The migration of ECs is required for vascular repair to avoid thrombosis in large vessels and to minimize tissue ischemia in the microcirculation.[2] Therefore understanding the environmental factors that modulate and evaluate ECs migration is critical towards the development of novel methods for vascular therapy.[2] Focal adhesions (FAs), the cytoskeleton, and intracellular signaling molecules in migrating ECs must respond to a variety of environmental signals and put them into coordinated intracellular responses that lead to cell migration. This

migration process includes morphological polarization, membrane extension, formation of cell substratum, contractile force and traction, and release attachments.[3]

2. Artificial blood vessel

Cardiovascular disease is a main reason of mortality and morbidity in most developed countries.[4] When it is impossible to treat the diseased blood vessels using drug or operation, or when the blood vessel is damaged by the accident, we need the artificial blood vessels to replace damaged and diseased blood vessels.

Current synthetic grafts are widely based on expanded polytetrafluoroethylene (ePTFE) or polyethylene terephalate (Dacron).[5] Regarding artificial blood vessels for replacing damaged or diseased blood vessels, large-diameter artificial blood vessels (>5mm) have already performed successfully, but the small-diameter artificial blood vessels (<5mm) are highly associated with thrombosis and intimal hyperplasia after grafting.[6, 7] These may lead to fail of small-diameter artificial blood vessels. Loss of the endothelium at the prosthetic graft site may be significant to increase intimal hyperplasia at the site. Rapid re-endothelialization of the arterial wall as well as endothelialization of the injured site in the prosthetic surface are, therefore, crucial for the prevention of thrombosis and for constant patency.[8] Unless endothelial cells from another source are somehow introduced and seeded at the site, coverage of an wounded part of endothelium is completed largely, at least initially, by migration of endothelial cells from near vessel areas of undamaged endothelium.[8]

3. Mechanotaxis

The chemical and physical factors in the vascular system regulate ECs migration by different mechanisms. One of these mechanisms is mechanotaxis that induces directional migration in response to mechanical forces.[9] *In vivo*, ECs are continually exposed to fluid shear stress, the tangential component of hemodynamic force because of blood flow (Fig. 1). Shear stress has been found to remodel ECs monolayer that induces the mechanism of the signal transduction and gene expression[10] and increase stress fibers.[11] While shear stress is applied on the luminal surface of ECs, the mechanical-chemical signaling can be transmitted throughout the cell and to cell extracellular matrix (ECM) adhesions on the abluminal surface of ECs. There is accumulating evidence suggesting that fluid shear stress can modulate each step of the migration process, including the extension of the leading edge, adhesion to the matrix, and release of adhesions at the rear.[9] The rate and extent of endothelial migration onto a prosthetic material vascular stent surface are influenced by the level and direction of flow-related wall shear stress[8, 12] , but the kinetics and molecular mechanism of EC migration in response to shear stress remain to be determined.

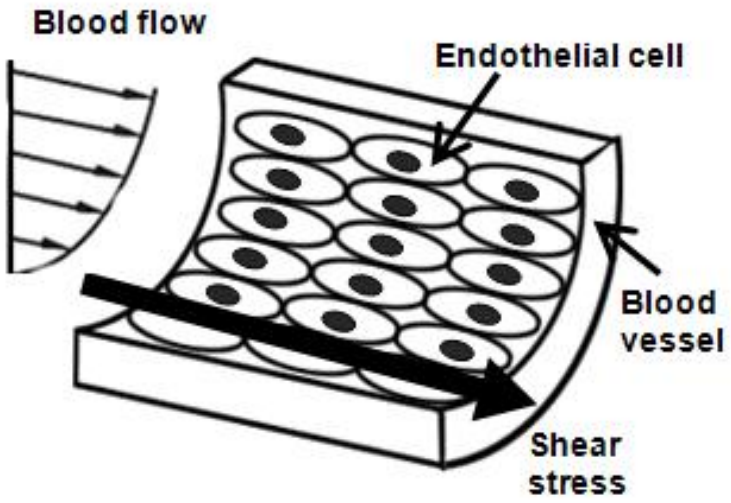

Figure 1. Arterial wall showing endothelial cell and blood flow

4. Scaffold for tissue engineering

Tissue engineering is a promising technology that applies the principles of biology and engineering to the development of functional substitutes for injured tissue.[13] One method to tissue engineering is to isolate cells, culture the cells *in vitro*, and seed them into an artificial structure that is able to support three dimensional (3D) tissue formations. This 3D structure is called scaffold. It is known that a porous scaffold is required to allow cell seeding or migration throughout the pore. Therefore, pore size is critical for tissue development and determines the inner surface area for cell attachment.[14]

In these processes, cell is seeded at first step to form the 3D tissue-like structures. However, it is technically difficult to seed the cells to scaffold. One reason is insufficient migration into the scaffolds because of pore size and material.[15] Therefore, various methods for effective cell seeding into 3D scaffolds have been examined.

5. Objectives of this study

The purposes of this study are to evaluate effects of shear stress on endothelial cells *in vitro* and to analyzes the migration of ECs such as cell movement speed, directionality and X forward migration index. To investigate the migration of ECs, we utilized a parallel plate flow chamber system to apply a shear stress of physiologically equivalent magnitude to a monolayer of ECs grown on a gelatin coated coverslip. Also, immustatining was carried out to confirm the focal adhesion and actin cytoskeleton alignment. Finally we studied cell migration into scaffold in response of flow using flow perfusion system.

II. Materials and methods

1. Cells and cell cultures

Human umbilical endothelial cells (HUVECs) were purchased from Cambrex Bio Science Walkersville. These cells were cultured in Endothelial basal medium-2 (EBM-2, Lonza, Walkersville, MD, USA) supplemented with 2 % fetal bovine serum (FBS, Lonza) and endothelial cell growth factors (Lonza, Hydrocortisone 0.2 ml, hFGF-B 2 ml, VEGF 0.5 ml, R3-IGF-1 0.5 ml, Ascorbic acid 0.5 ml, hEGF 0.5 ml, GA-1000 0.5 ml, Heparin 0.5 ml). Before cells were seeded, 18 mm round coverslips (Fisherbrand, Leicestershire ,United Kingdom) were coated with 0.2 % gelatin (Gelatin from porcine skin Type A, sigma). Before using the coversilp, it was dipped into 100 % ethanol and flame sterilized. 500 ul of 2 % gelatin solution in phosphate buffered saline (PBS) was added to 18 mm coverslips and incubated for 2 hours at 37 ℃. After 2 hours, 2 % gelatin solution was suctioned and dried in air. The cells were plated onto gelatin-coated coverslips and were incubated for 24 hours before exposure to flow. HUVECs were studied before passage 10 in all experiments.

2. Cell seeding models

There are two models of cell seeding, wound closure model and individual cell migration model. For wound closure experiments, we used the silicon culture insert (Ibidi, Mnchen, Germany) to form well-defined denuded zones. Silicon culture insert consisted of two individual wells for cell seeding. After culture insert put on the coverslip, 8 x 10^3 cells in 100 ul were plated on each well confluently and homogenously. 24 hours after cell attachment, the culture

insert was removed and we could observe cell-free area. The wound width was approximately 500 um. The shear stress was applied in the direction of perpendicular to flow. For individual cell migration model (nonconfluent), 8 x 10^3 cells in 600 ul were plated on the coverslip at 30 % confluency.

3. Parallel plate chamber system

We used the parallel plate chamber system (Fig. 2) to apply shear stress to HUVECs. The parallel plate chamber system consisted of two parts, incubator system installed with the microscope to observe live cells and the flow chamber to apply shear stress to the cells. The incubator was regulated by temperature and gas composition controlling program (CCP ver. 3.8) under proper environment for cell (CO_2 5 %, 37 ℃). The flow chamber was made up by main body with inlet and outlet for tubing (inner diameter, 2 mm), bottom plate and silicon gasket. Gelatin-coated coverslip seeding HUVECs was mounted on the bottom plate and put the main body and the silicon gasket (200 um in height, 2 mm in width) together. Medium was taken out at least for 1 hour before starting experiments to prevent bubbles. In case of wound closure experiments, the flow was applied in a direction perpendicular to the wound. Upstream is the same direction of flow and cell movement while downstream is the opposite direction of flow and cell movement. The shear stress (dyne/cm^2) was calculated by this equation.

$$\tau = 6Q\mu/Wh^2.$$

Q is the volumetric flow rate (ml/s), μ is the viscosity of the medium (dyne.s/cm^2), .W is the gasket width (cm) and h is the gasket height (cm).[2] It was known that physiological levels of venous and arterial shear stresses are 1-5 and 6-40 dynes/cm^2, respectively.[12] Thus, we selected 4 and 8 dyne/cm^2 in the physiological level of shear stress. Moreover, blood flow is pulsatile due to the

heart beat through the arteries, thus we need to mimic the condition of pulsatile flow. To explore the effects of pulsatile flow on the endothelial cells, we used peristaltic pump that produces 60 cycles/min. In contrast, in steady flow conditions, we used the syringe pump.

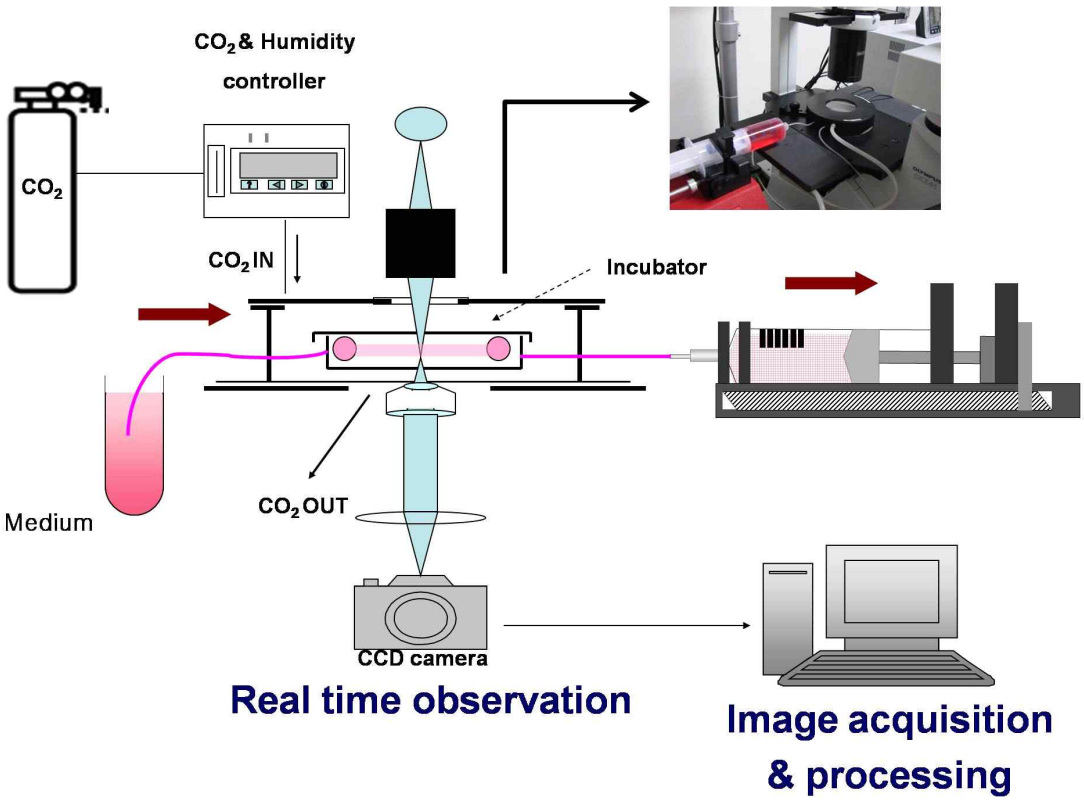

Figure 2. Schematic diagram of the parallel-plate flow chambers in a flow system for the evaluation of the cell migration.

4. Immunostaining

The dynamic assembly and disassembly of focal adhesions (FAs) plays a central role in cell migration.[17] Vinculin is related with focal adhesion and adherens junctions, which are complexes that nucleates actin filaments and crosslinks between the external medium, plasma membrane, and actin cytoskeleton.[18] Immunofluorescence staining of vinculin was performed to visualize focal adhesions. After applying shear stress for 30 minuts and 5 hours, vinculin for focal adhesions, actin cytoskeleton and nucleus were visualized by immunostaining. Each step for immunostaining was as following. Cells were fixed with 3.7 % paraformaldehyde for 15 min at room temperature and were washed two times with PBS. Cells were permeabilized with 0.25 % Triton X-100 in PBS for 5 min at room temperature and rinsed 3 times with PBS. Nonspecific bindings to cells were blocked with 1 % bovine serum albumin (BSA) for 30 minutes at room temperature, followed by and incubated with anti-vinculin primary antibody (dilution 1:60, Santa Cruz Biotechnology, Santa Cruz, CA, USA) overnight at 4 ℃. Cells were then washed three times with PBS for 5 minutes on the shaker. In dark, they were treated with secondary antibody, goat anti-mouse IgG conjugated with Texas Red (dilution 1:100, Santa Cruz, CA, USA) for vinculin staining, Hoechst #33258 (dilution 1:1000) for nucleus staining and Alexa (488)-conjugated phalloidin (5 U/ml, Invitrogen) for actin cytoskeleton staining for 30 min at room temperature. The monolayers were mounted under a coverslip with aqueous mounting medium (Dako Faramounts, Dako North America Inc., CA, USA) and were observed by a fluorescence inverted microscope.

5. Time-lapse phase contrast microscopy and Analysis of cell migration.

A. Image acquisition

The cells were cultured in the incubator placed on the microscope stage. and cell images were recorded every 5 minutes for 8 hours by the change-coupled device (CCD) camera (Electric Biomedical Co. Ltd., Osaka, Japan) attached to the inverted microscope (Olympus Optical Co. Ltd., Tokyo, Japan). Images were conveyed directly from a frame grabber to computer storage using Tomoro image capture program and memorized them as JPEG image files.

B. Cell tracking and evaluation of cell migration

For data analysis, captured images were imported into ImageJ (ImageJ 1.37v by W. Rasband, National Institutes of Health, Baltimore, Md). Image analysis was carried out by manual tracking and chemotaxis and migration tool plug-in (v. 1.01, distributed by ibidi GmbH, Mnchen, Germany) in ImageJ software. We obtained the datasets of XY coordinates by using manual tracking. Then, these datasets were imported into chemotaxis and migration tool plug-in. The tool computed the cell migration speed, directionality and X forward migration index (X_{FMI}) of HUVECs and plotted cell migration pathway. The migration speed was calculated as an accumulated distance of the cell divided by time. The directionality of the cell was defined as an Euclidean distance divided by accumulated distance.The Euclidean distance means the straight-line distance between the start point and the end point.(Fig. 3A) The closer the directionality was to 1, the straighter the cell moved. The X_{FMI} of the cell was defined as an

X_{FMI} divided by accumulated distance.(Fig. 3B) For each experiment, 20 cells were randomly selected along each edge of the wound. Cells undergoing division, death, or migration outside the field of view were excluded from the analysis.

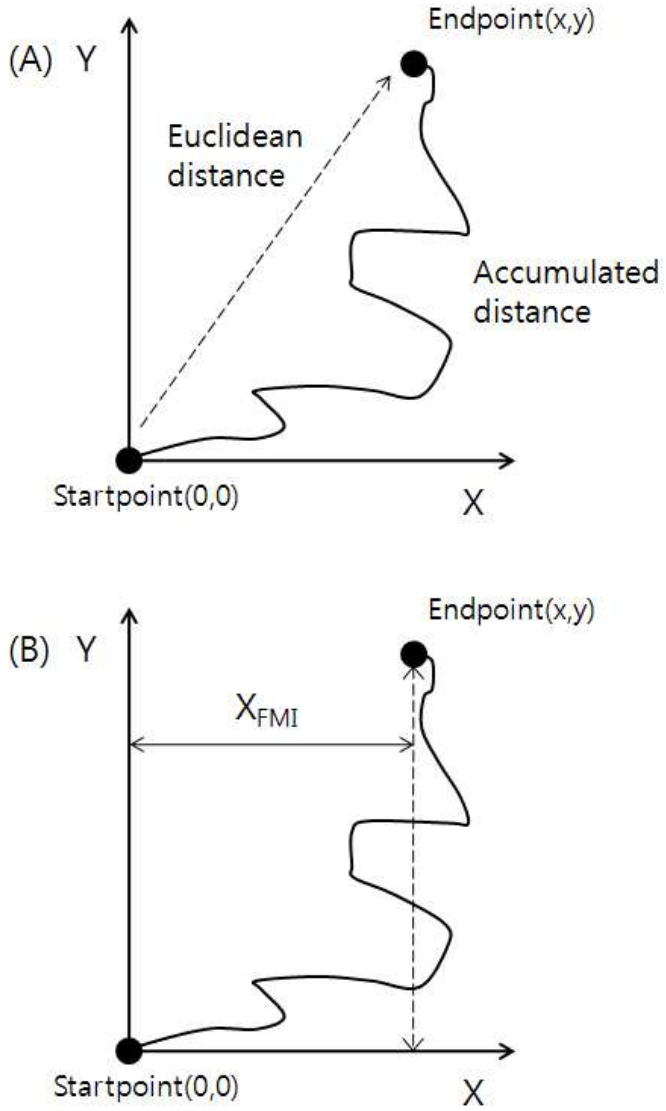

Figure 3. The evaluation of cell migration (A) Schematic of accumulated distance and Euclidean distance of cell movements. (B) X forward migration index (X_{FMI})

6. HUVECs migration into scaffold in response of flow

A. PLLA scaffold

We were provided with the scaffold from Ehwa Woman university. Poly (L-lactic acid) (PLLA) (intrinsic viscosity 0.63 dl/g, Mw = 2.5 x 10^5 g/mol) was provided by Purac Biochem (Gorinchem, Netherlands). Dichloromethane (MC) and acetone were purchased from Duksan Chemicals Co. (Seoul, Korea). In brief, 8 % w/v PLLA solutions were prepared with the solvent mixture composed of MC and acetone (90:10 v/v). The polymer solution was poured into a 10-mL glass syringe, attached to a 25-gauge blunt end needle. A syringe pump was set at a volume flow rate of 0.1 ml/min. The distance between the needle tip and the collector was 15 cm. The electrospinning process was carried out in a sterile environment at high voltage. A voltage between 8 and 20 kV was used for all solutions. Prior to usage, the electrospun scaffolds were dried for three days under a vacuum at 70 ℃ to remove the solvents. (Fig. 4B)

B. Cell seeding of scaffold

HUVECs were cultured in the way of 2D static culture at 37 ℃ and 5 % CO_2. EBM-2 (Lonza, Walkersville, MD, USA) supplemented with 2 % fetal bovine serum (FBS, Lonza, Walkersville, MD, USA) and endothelial cell growth factors (Lonza, Hydrocortisone 0.2 ml, hFGF-B 2 ml, VEGF 0.5 ml, R3-IGF-1 0.5 ml, Ascorbic acid 0.5 ml, hEGF 0.5 ml, GA-1000 0.5 ml, Heparin 0.5 ml) was used. When cells reached confluency, they were detached using 0.25 % trypsin-EDTA (Welgene Inc., Daegu, South Korea), resuspended with the same medium and seeded the scaffold. HUVECs were studied before passage 10 in

all experiments

Microfibrous scaffolds of weigh 80 mg were prepared and each of these was placed in a separate well of a 24 well tissue-culture plate for cell seeding. To remove their hydrophobic characteristic and to sterilize them, scaffolds were dipped into 70 % ethanol for over 10 minutes and washed 2 times with PBS. The cells were seeded onto scaffold at a concentration of 1 x 10^5 cells of each scaffold. After incubating for 4 hours to allow cell attachment, cell-seeded scaffolds were either placed in flow perfusion culture or continued in static culture.

C. The flow perfusion system

We used the peristaltic pump that produce 500 ml/hour to circulate the medium. The chamber was tapered to ensure flow from the outer edges of the scaffold as well as the center to the exit port of the chamber. Screw caps were fitted with O-rings for a tight seal and preventation of leakage. The peristaltic pump pulled medium from the reservoir and provided it to the chamber including cell-seeded scaffold via 6 mm inner diameter silicone tubing. Equipment was sterilized by steam autoclave (tubing, chamber). The apparatus was assembled under sterile conditions in a laminar flow biosafety cleanbench. In order to incubate the cells in the chamber, a CO_2 mini-incubator (150x130x40 mm) was designed and fabricated with a double-layered acrylic plate. The mini-incubator was connected with a CO_2 gas mixing system (FC-5, Live cell instrument Inc., Seoul, Korea) and supplied 5 % CO_2. (Fig.4A)

D. Observation of cells distribution in scaffold

After 4 hours seeding the cells, the scaffolds were washed 2 times with PBS and the cells were fixed with pre-cooled (-20 ℃) 70 % ethanol for 5 minutes. Then, the cells were stained with propidium iodide (Sigma, Steinheim, Germany). The migration of cells into the scaffold was calculated by a confocal microscope (LSM 510, Carl Zeiss Micro Imaging Inc., North America), using horizontal and vertical sections through the scaffolds every 10 um.

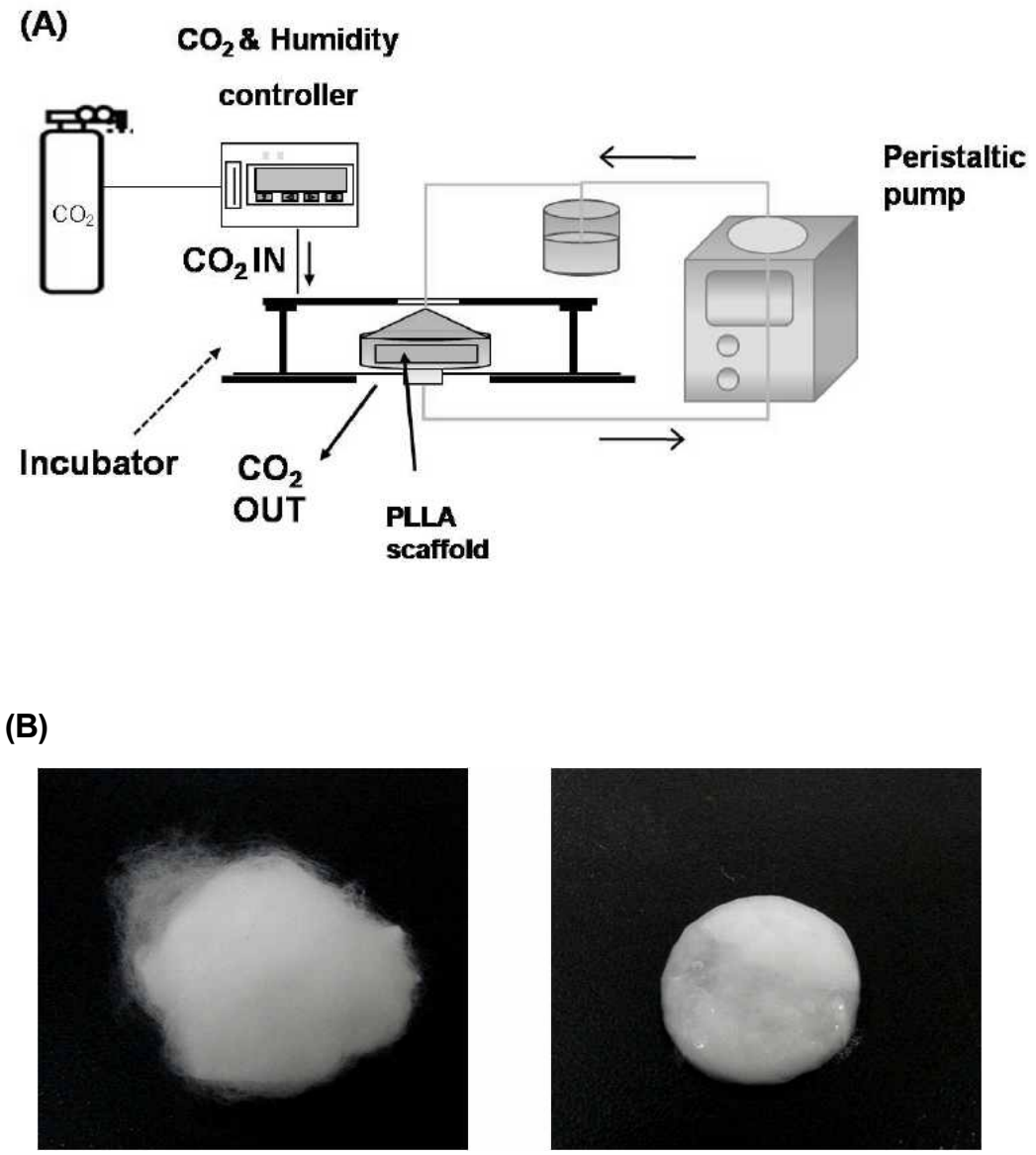

Figure 4. **HUVECs migration into scaffold in response of flow.** (A) Schematic diagram of the flow perfusion system for the evaluation of the cell migration into the scaffold. (B) Microfibrous PLLA scaffold. Microfibrous scaffolds of weigh 80mg were prepared (left) and each of these was placed in a separate well of a 24 well tissue-culture plate for cell seeding (right).

7. Statistical analysis

All statistical analyses were completed with SPSS Software version 12.0 (SPSS, Chicago, IL, USA). Non-normal distributions in the data were not allowed to use Analysis of variance (ANOVA) and t-tests. Therefore, comparisons between groups were carried out using the nonparametric Kruskal-Wallis test. Comparisons between subgroups used the Mann-Whitney U test with Bonferroni correction for multiple comparisons, thus yielding statistical significance if $p < 0.0167$. All data were presented as mean values and standard deviation (SD).

III. Result

1. Movement of HUVECs in accordance with the shear stress in the wound closure model.

Before exposure to the shear stress, HUVECs were seeded using the silicon culture insert to form clear denuded zone. Twenty four hours after cell attachment, flow was applied perpendicular to the wound axis. A denuded zone into an endothelial cell monolayer produced polarization of cells and migration into the wound.[19]

Under static condition, the cells along both edges of the wound migrated at the same speed and directionality to cover the wounded area. When the monolayer were subjected to shear stress, the cells along the downstream edge migrated significant slower than cells along the upstream edge. Surprisingly, the migration speeds of the cells along the upstream edge in response to shear stress were not larger than those under static conditions (Fig. 5A).

In case of directionality, the cells moved in a similar straight in downstream part in regardless of shear stress. Although the cells moved considerably straight in upstream part after shear stress, there is no significant difference between 4 dyne/cm^2 and 8 dyne/cm^2 (Fig. 5B).

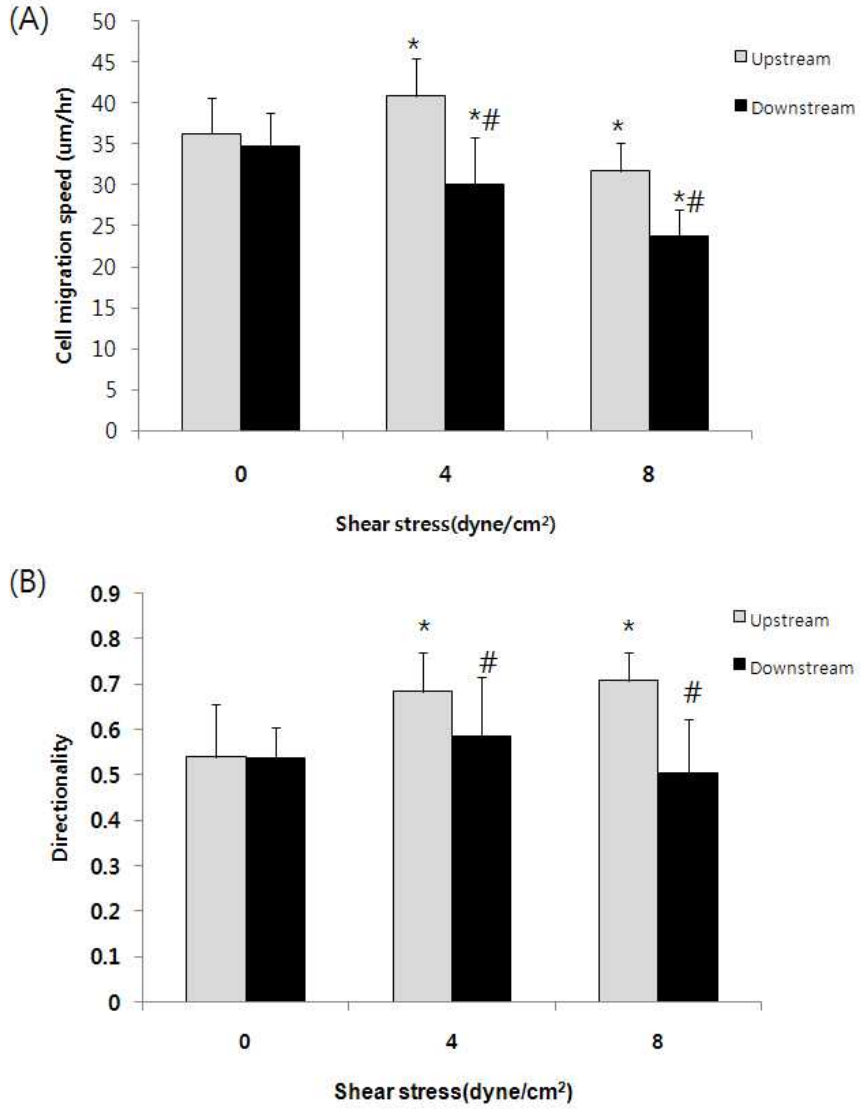

Figure 5. Movement of HUVECs in accordance with the shear stress in wound closure model. (A) The migration speed of HUVECs. (B) The directionality of HUVECs. Analyzed by Mann-Whitney U test and statistical significance was considered as $p < 0.0167$. These results were derived from measurements on 30 cells from 3 separate experiments. Values were means ±SE. The results are shown as a mean standard deviation (n = 30). * $p < 0.0167$ compared with static condition (0 dyne/cm^2), # $p < 0.0167$ compared with upstresam part.

2. Directional migration of HUVECs in the wound closure model.

We examined X forward ECs migration index that is perpendicular to the wound as the proper assessment of wound healing process. As we mentioned, all experiments were performed to attach cells onto gelatin-coated coverslip for 24 hours before exposure of shear stress and observed for 7 hours.

Fig. 6 showed that under static condition, the X_{FMI} after wounding was approximately the same for cells along both edges. After flow was applied, cell migrated in the direction of flow. The X_{FMI} was significantly higher under flow condition in upstream edge than that observed in the absence of flow. The direction of cell migration in downstream part was usually opposite direction to flow compare with the static condition, because they moved to close wound area. In results, shear stress inhibited cell migration in the direction to the wound area in downstream part.

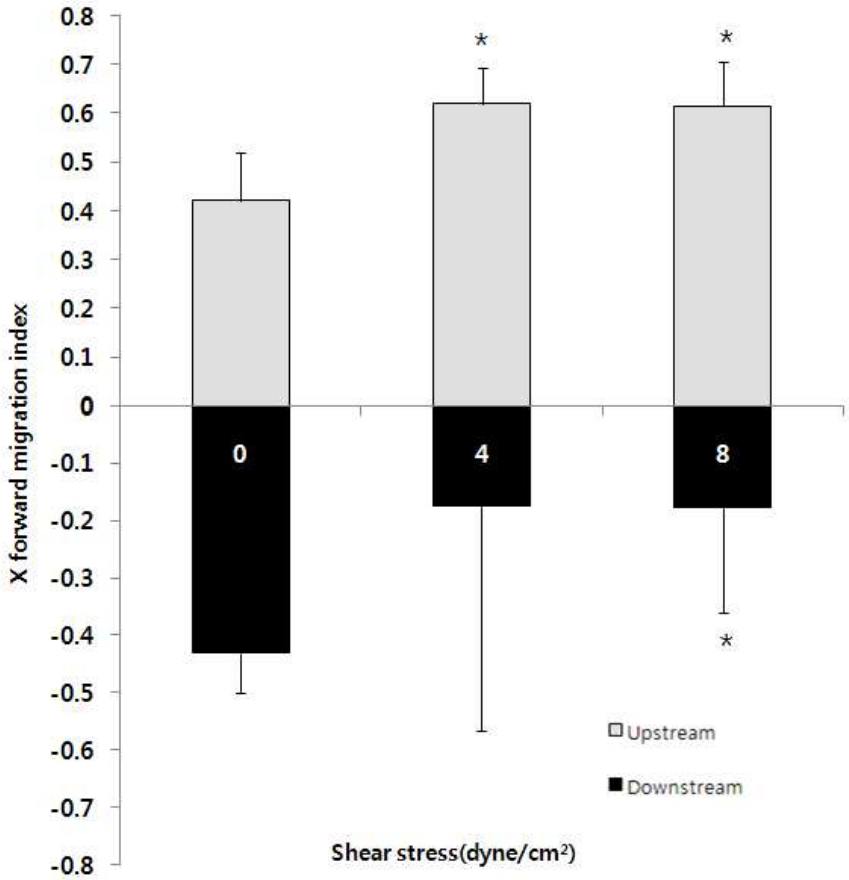

Figure 6. Directional migration of HUVECs in wound closure model. Analyzed by Mann-Whitney U test and statistical significance was considered as $p < 0.0167$. These results were derived from measurements on 10 cells from 3 separate experiments. Values were means ±SE. The results are shown as a mean standard deviation (n = 30). * $p < 0.0167$ compared with static condition (0 dyne/cm^2)

3. Movement of HUVECs in accordance with the shear stress in the individual cell migration model.

We characterized the migration speed of the ECs under static and flow conditions.(Fig. 7) Subconfluent HUVECs were plated on gelatin-coated cover slip and were then kept as static controls or subjected to shear stress at 4 and 8 dyne/cm^2. Cell movement was monitored by time-lapse microscopy and time-lapse images were tracked every 5 minutes for 7 hours after cell seeding to evaluate the migration speed and the directionality of cells. The closer the directionality was to 1, the straighter the cell moved.

The application of shear stress significantly increased the cell migration speed. In case of the directionality, HUVECs moved more straightly under flow condition compared to the static condition.

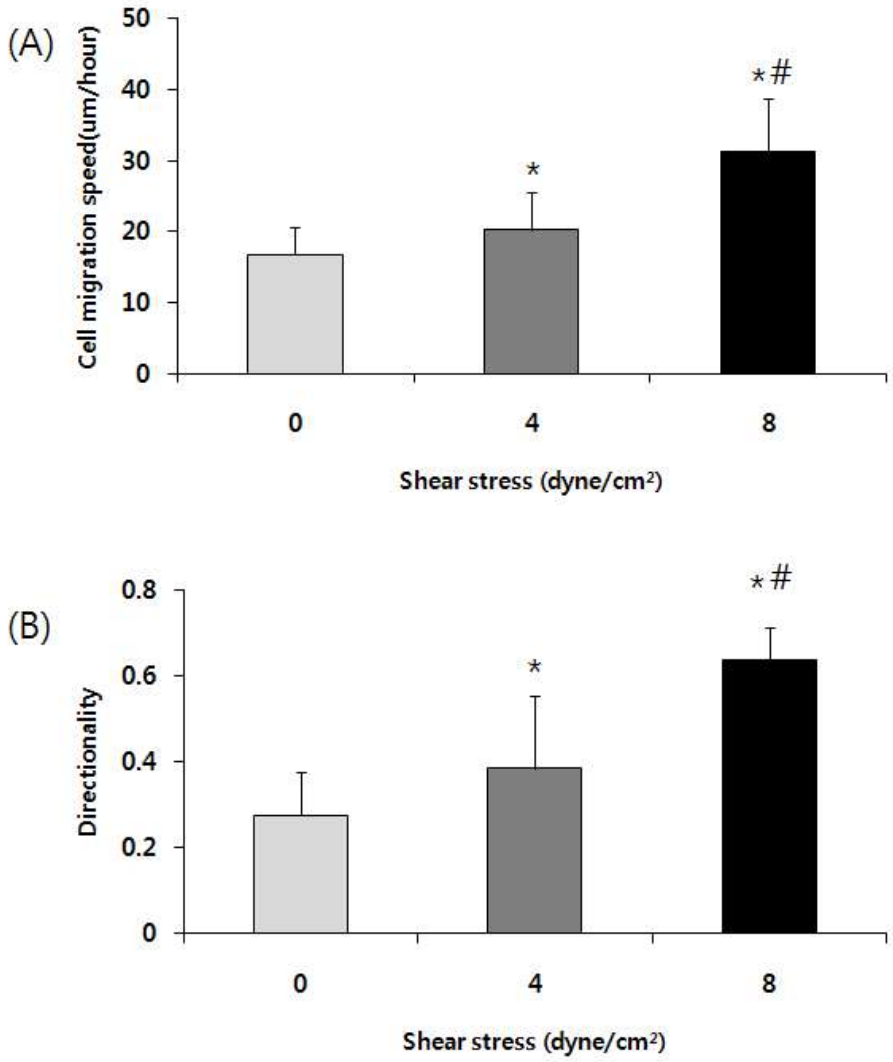

Figure 7. Movement of HUVECs in accordance with the shear stress in individual cell migration model. (A) The migration speed of HUVECs. (B) The directionality of HUVECs. Analyzed by Mann-Whitney U test and statistical significance was considered as $p < 0.0167$. These results were derived from measurements on 10 cells from 3 separate experiments. Values were means ±SE. The results are shown as a mean standard deviation (n =30). * $p < 0.0167$ compared with static condition (0 dyne/cm^2), # $p < 0.0167$ compared with 4 dyne/cm^2.

4. Directional migration of HUVECs in individual cell migration model.

To assess the effect of shear stress has on x directional migration of HUVECs, after tracking the cell movement using manual tracking in ImageJ, x directional migration was calculated as the ratio of the net distance that the cell migrated in the forward direction to the total migration length that the cell traveled.

When HUVECs were seeded randomly and nonconfluently, they did not tend to move in the direction of flow under stactic condition and 4 dyne/cm^2. X_{FMI} between static condition and 4 dyne/cm^2 was not significantly different (Fig. 8A). But when HUVECs were subjected to shear stress at 8 dyne/cm^2, they started moving in the direction of flow (Fig. 8B). X_{FMI} at 8 dyne/cm^2 moved significantly in the direction of flow than in the absence of flow.

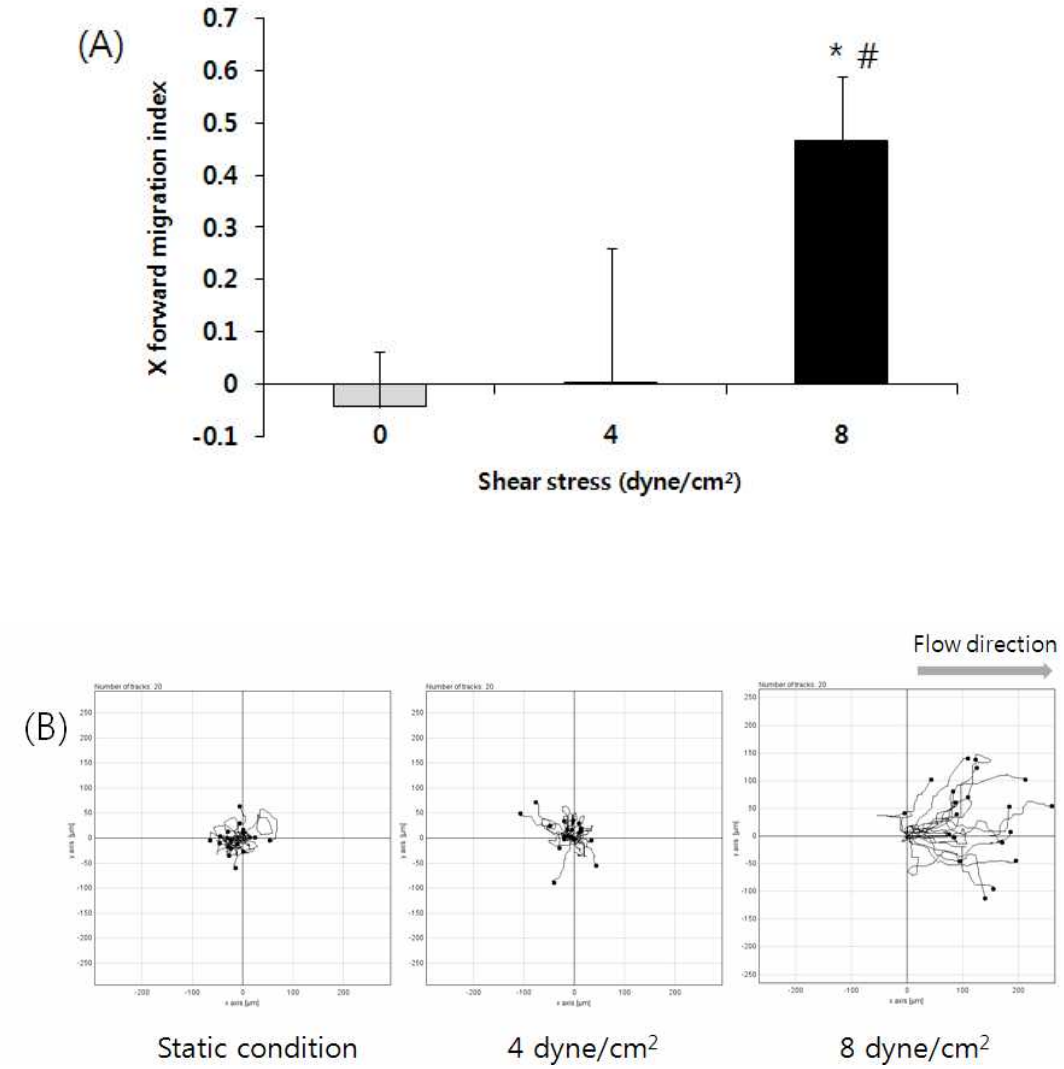

Figure 8. The directional migration of HUVECs in individual cell migration model. (A) X_{FMI} of HUVECs. Analyzed by Mann-Whitney U test and statistical significance was considered as $p < 0.0167$. These results were derived from measurements on 10 cells from 3 separate experiments. Values were means ±SE. The results are shown as a mean standard deviation (n = 30). * $p < 0.0167$ compared with static condition (0 dyne/cm^2), # $p < 0.0167$ compared with 4 dyne/cm^2. (B) Trajectories of HUVECs. During 7 hours all cells were assumed to originate at (0,0) under static conditions and fluid shear stress (4 dyne/cm^2, 8 dyne/cm^2). The movement of 20 cells is shown.

5. Laminar flow vs Pulsatile flow

Fluid shear stress was generated by the syringe pump and the peristaltic pump. The syringe pump produced laminar flow constantly. While the peristaltic pump produced pulsatile flow at 60 cycles/min that was more similar to human body condition. The shear stress was set up at 8 dyne/cm^2 both of them and analyzed cell migration speed, directionality and X_{FMI}.

In Fig. 9 result, there were no significant difference in cell migration speed and directionality under pulsatile flow and laminar flow. On the other hand, HUVECs significantly moved more in the direction of the flow under pulsatile flow compared with laminar flow.

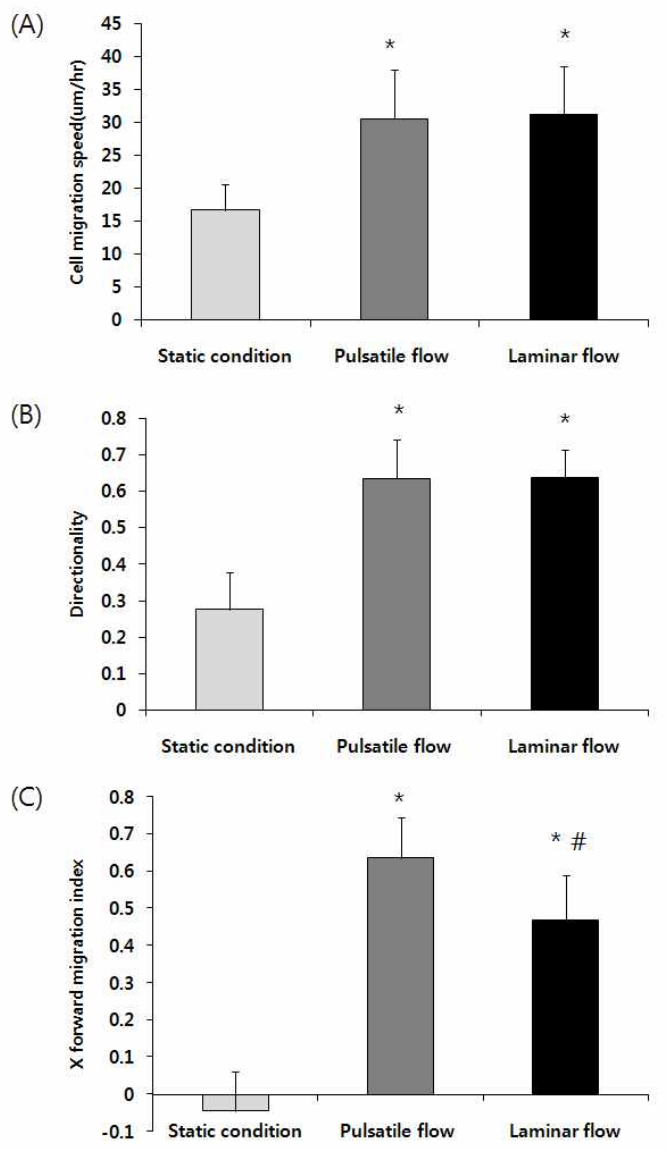

Figure 9. Comparision with cell migration under pulastile flow and laminar flow. (A) Cell migration speed (B) Directionality (C) X_{FMI}. All experiments were carried out at 8 dyne/cm^2. Analyzed by Mann-Whitney U test and statistical significance was considered as $p < 0.0167$. These results were derived from measurements on 10 cells from 3 separate experiments. Values were means ±SE. The results are shown as a mean standard deviation (n = 30). * $p < 0.0167$ compared with static condition (0 dyne/cm^2), # $p < 0.0167$ compared with pulsatile flow.

6. Focal adhesion formation and actin cytoskeleton alignment

HUVECs were kept as static controls and subjected to a shear stress of 8 dyne/cm^2 for 30 min and 5 hours with the direction of flow from the left to the right. Cells were then fixed and immunostained with anti-vinculin primary antibody and Alexa (488)-conjugated phalloidin.

Fluorescent images of actin cytoskeleton, vinculin and nucleus were shown in Fig. 10 for statically cultured cells and in Fig. 11, Fig. 12 for sheared cells. Under static condition (no flow), endothelial cells showed a cobblestone structure with a quite rounded shape. (Fig. 10) Also focal adhesions and actin cytoskeleton formed without preferred direction.(Fig. 10A, Fig. 10B) Fig. 8 showed the effect of flow direction on morphological responses of HUVECs at shear stress of 8 dyne/cm^2 for 5 hours. HUVECs under the flow conditions remodeled their actin cytoskeleton in the direction of applied flow (Fig. 11A). Previously many studies have shown that shear stress induces lamellipodial protrusion and FAs formation in the flow direction.[20, 21] This could result in EC migration. We observed the increase of focal adhesions at the leading edge in the direction of flow. (Fig. 12B)

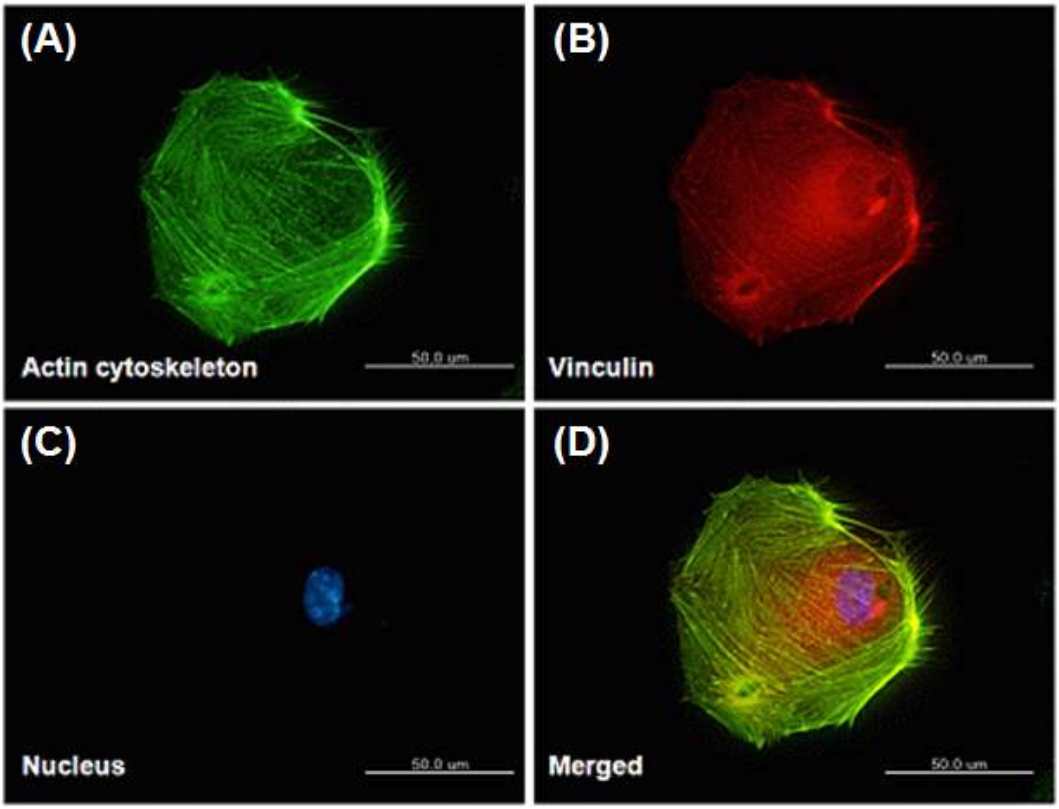

Figure 10. Immunostaining of vinculin, actin cytoskeleton and nucleus under static condition (A) Vinculin was stained with Texas Red conjugated antibody (red) and (B) Actin cytoskeleton was stained with Alexa (488)-conjugated phalloidin (green) and (C) Nucleus was stained with Hoechst #33258 and (D) merged imaged were shown. Scale bar = 50um

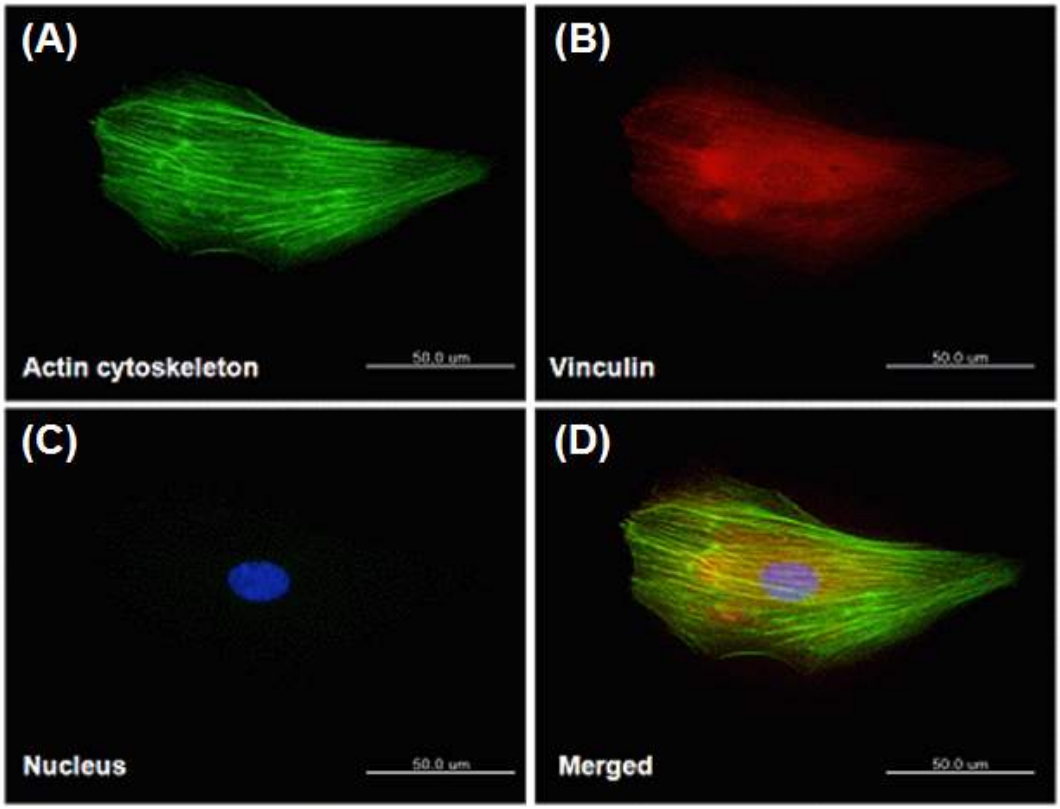

Figure 11. Immunostaining of vinculin, actin cytoskeleton and nucleus under flow condition. Shear stress of 8 dyne/cm^2 was applied for 5 hours (A) Vinculin was stained with Texas Red conjugated antibody (red) and (B) Actin cytoskeleton was stained with Alexa (488)-conjugated phalloidin (green) and (C) Nucleus was stained with Hoechst #33258 and (D) merged imaged were shown. Scale bar = 50um

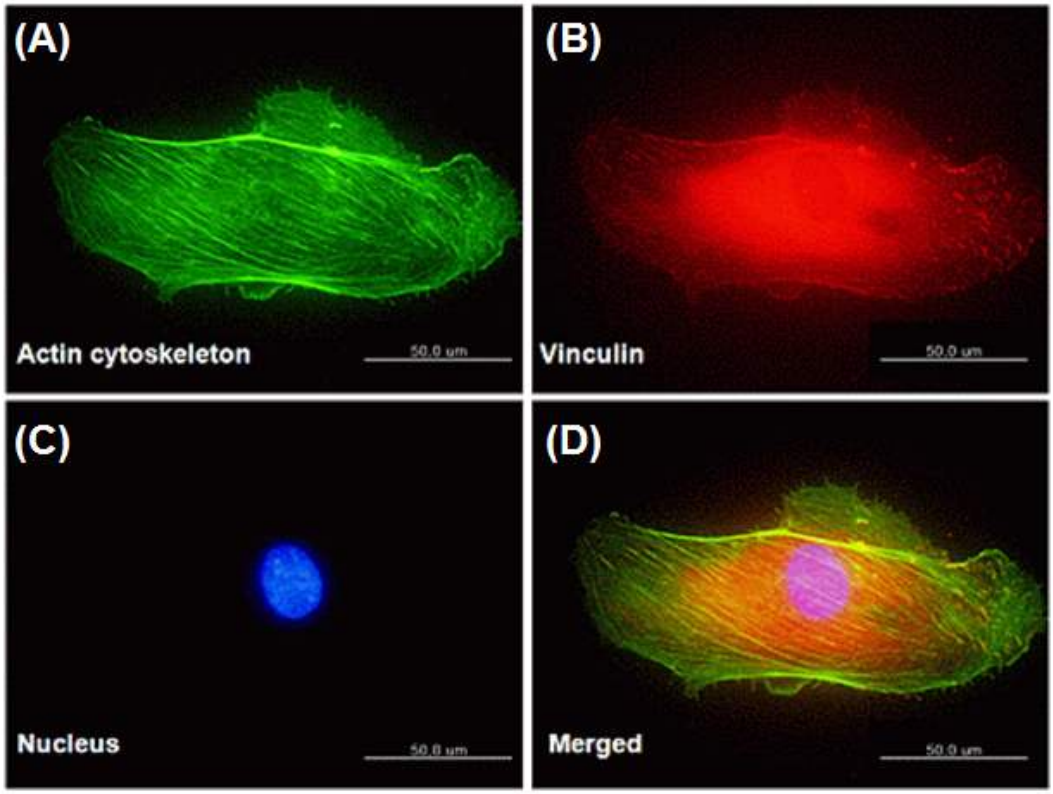

Figure 12. Immunostaining of vinculin, actin cytoskeleton and nucleus under flow condition. Shear stress of 8 dyne/cm^2 was applied for 30 minuts (A) Vinculin was stained with Texas Red conjugated antibody (red) and (B) Actin cytoskeleton was stained with Alexa (488)-conjugated phalloidin (green) and (C) Nucleus was stained with Hoechst #33258 and (D) merged imaged were shown. Scale bar = 50um

7. HUVECs migration into scaffold in response of flow

The flow perfusion system was set up for effective cell seeding into the 3D scaffold in the based on the previous data. Microfibrous scaffolds of weigh 80 mg were placed in each 24 well tissue-culture plate. Four hours after cell seeing onto scaffolds and attachments, cells were cultured under static and flow condition. In results, under static condition, cells could not invade into microfibrous scaffold. Thus, cell tended to remain in the upper part.(Fig. 13A) Even though cells were cultured for longer time, they did not invade into the scaffold.(Fig. 13B) On the other hand, under flow condition, cells penetrated into scaffolds more than at the static condition. (Fig. 13C, Fig. 13D, Fig. 14)

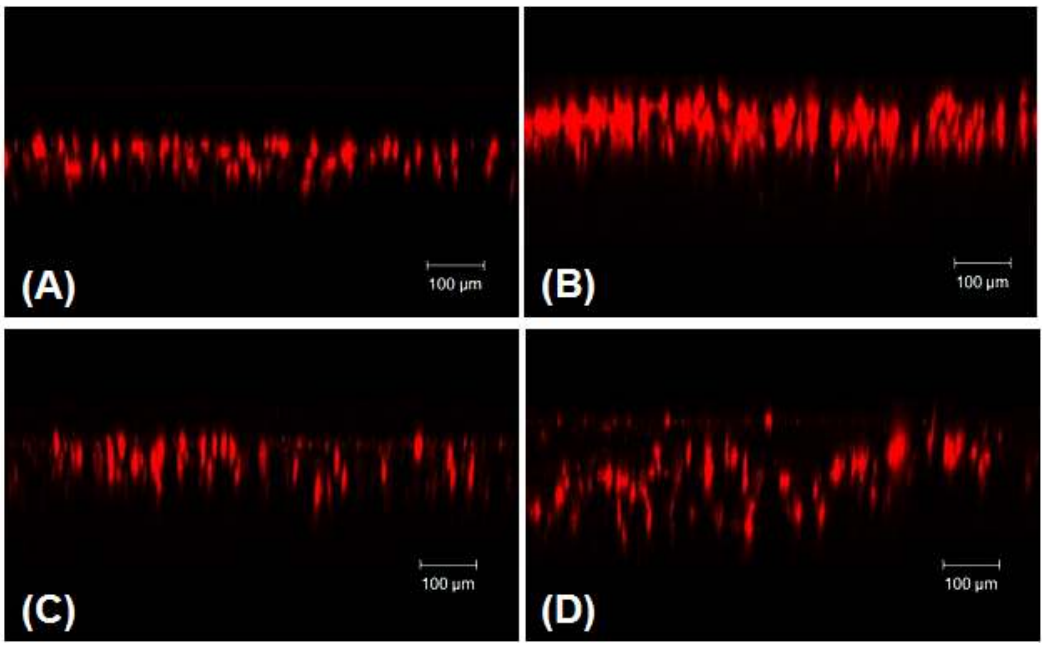

Figure 13. Cross sectional area of confocal image for cell invasion into Scaffold. (A) under static condition for 12hr. (B) under static condition for 24hr. (C) Under flow condition for 12hr (D) Under flow condition for 24hr. Scare bar = 100 um

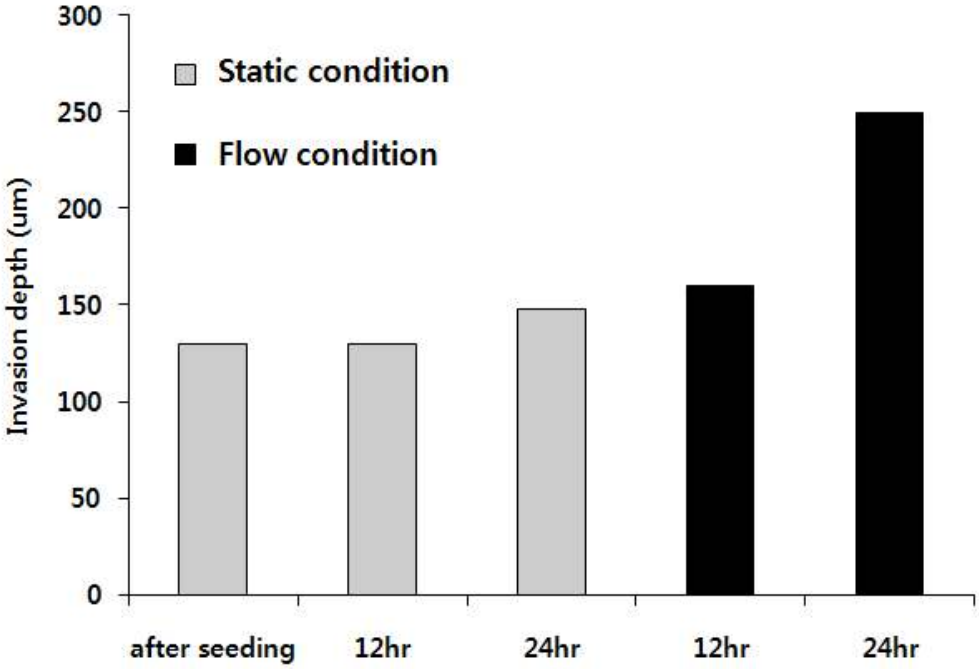

Figure 14. The invasion depth of HUVECs into scaffold in response of flow. Cells penetrated into scaffolds more than the static condition under flow condition.

IV. Discussion

In this study, we confirmed the possibility to observe cell migration under static and flow condition using the parallel plate chamber system and to analyze the cell migration speed, directionality and X_{FMI}.

Experiments were conducted in two models of cell seeding. They were the wound closure model and the individual cell migration model. Usually they have different environment for cell culture.

To perform the wound closure model, the silicon culture insert was used to create the wound area clearly. The wound closure model induced cell migration into wound area. ECs migration and proliferation has been related to the primary mechanism for the regeneration of the wounded endothelial monolayer under static conditions.[22, 23] Endothelial cells *in vivo* are exposed to continual flow and must bring about wound closure under conditions of shear stress. It is important to examine the effect of shear on endothelial cell spreading, migration, but not proliferation.[24, 25] Thus, cell spreading and migration seems to be the major mechanism for the *in vitro* EC wound closure under shear condition.

Upstream is the same direction of flow and cell movement while downstream is the opposite direction of flow and cell movement. In this study, the result showed that shear stress inhibited cell migration in the direction to the wound area in downstream part. On the other hand, the cells in the upstream part more migrated into the wound area under flow condition compared with in the absence of flow. The level of shear stress we chose in this report retarded the wound closure rate even though the cells in upstream part migrated straight and fast in the direction of flow. Lamellipodial protrusions were restricted to the downstream part of cells and actin and vinculin showed that focal complexes

are restricted to the downstream side of cells, whereas the upstream region contained large focal adhesions.[26]

For the individual cell migration model, endothelial cells were sparsely plated on coverslips at 30 % confluency. This model is appropriate for observing single cell migration. The application of shear stress significantly increased the cell migration speed and cells moved more straightly under flow condition compared to under static condition. The process of adaptation of sparse endothelial cells to shear stress can be divided into two stages regulated by RhoA, Rac1, and Cdc42.[27] The Rho GTPases Rho, Rac and Cdc42 play several roles in migrating endothelial cells.[28,29] In the first stage, an increase in RhoA activity leads to the formation of stress fibers and cell contraction. This allows cells to elongate efficiently in the direction of shear stress. This elongation involves directional spreading via protrusion at the front of the cells, and is mediated by Rac and Cdc42 activation. Importantly, RhoA activity is down-regulated at this stage to allow optimal extension of protrusions. Later, RhoA activity increases, and Rho with Rac is required to maintain polarized migration in the direction of shear stress.[27]

Previous studies have reported that pulsatile flow affects endothelial cell function differently from steady flow, even though the average shear stress is the same.[30] For example, researchers have shown differences in intracellular calcium concentration[31], cell morphology[32], and endothelin mRNA levels.[33] As a result, there were no significant differences in cell migration speed and directionality under pulsatile flow and laminar flow. On the other hand, HUVECs significantly moved more in the direction of the flow under pulsatile flow compared with laminar flow. Pulastile flow may influenced the endothelial cells as previous studies mentioned.

It was shown in this research that endothelial cells experienced morphological changes when subjected to shear stress. Under static conditions, the cells were

characterized by round shape like cobblestone. However, an alteration in shape happened when a shear stress was applied. After the shear stress at 8 dyne/cm^2 for 5 hours, actin cytoskeleton looked more aligned in the direction of applied flow. Endothelial response of alignment and actin stress fiber induction in the direction of flow is dependent on intracellular calcium.[34] The result explained that actin cytoskeleton did not align in the direction of flow. Shear stress stimulated an increase of intracellular calcium. At first, calcium is released from compartments within the cell, and then later ion channels located on the cell membrane are opened allowing extracellular calcium to input.[35] As a result, signaling pathways associated with calcium may have function in the actin organization changes.

We observed the increase of FAs at the leading edge in the direction of flow after exposure of shear stress for 40 minutes. It is known that within 10 min of shear stress application, lamellipodial protrusions were induced at cell periphery in the flow direction, with the recruitment of focal adhesion kinase (FAK) at FAs. ECs under flow condition migrated with polarized formation of new FAs in flow direction, and these newly formed FAs subsequently disassembled after the rear of the cell moved over them.[36]

The flow perfusion system was established for effective cell seeding into the 3D scaffold. After cell seeding onto scaffolds and attachments, cells were cultured under static and flow condition. Under static condition, the result showed the cells located in the upper part. They could not enter the microfibrous scaffold. Although the cells were cultured for a longer time, they did not invade into the scaffold. However, when flow was applied to the scaffold, cells penetrated into it more than at the static condition.

Technical problems in cell seeding are produced by the complex structure of the scaffold[37, 38] and insufficient migration into the scaffolds caused by pore size and material, which prolongs the culture period because of the shortage of

initially seeded cells.[15] Therefore, a lot of effective seeding methods have been investigated[39] using different scaffolds such as meshes[40] and sponges or mixing conditions that is in static or mixed cultures.[41] This flow perfusion system may help to improve seeding efficiency and provide the uniform cell distribution throughout the matrix.

V. Conclusion

Shear stress was applied to endothelial cells using the parallel plate chamber and cell movements was characterized by image analysis program that measured the cell migration speed, directionality and X forward migration index. Also we examine that cells were allowed to migrate into scaffold using the flow perfusion system and finally help to provide the uniform cell distribution throughout the matrix.

These findings help us to predict the tendency of the cell migration *in vivo* under flow condition based on these *in vitro* results. It may allow to suggest stent designs or the structure of artificial blood vessels for proper re-endothelialization resulting from appropriate ECs migration.

References

1. Ohashi T, Sato M. Remodeling of vascular endothelial cells exposed to fluid shear stress: experimental and numerical approach. Fluid Dynamics Research 2005;37:40-59.
2. Hsu S, Thakar R, Liepmann D, Li S. Effects of shear stress on endothelial cell haptotaxis on micropatterned surfaces. Biochem Biophys Res Commun 2005;337:401-9.
3. Lauffenburger DA, Horwitz AF. Cell migration: a physically integrated molecular process. Cell 1996;84:359-69.
4. de Mel A, Bolvin C, Edirisinghe M, Hamilton G, Seifalian AM. Development of cardiovascular bypass grafts : endothelialization and application of nanotechnology. Expert Rev Cardiovasc Ther 2008; 6:1259-77.
5. Teebkenand OE, Haverich A. Tissue Engineering of Small Diameter Vascular Grafts. European Journal of Vascular and Endovascular Surgery 2002;23:475-85.
6. kannan RY, salacinski HJ, Butler PE, Hamilton G, Seifalian AM. Current status of prosthetic bypass grafts : a review. J Biomed Mater Res B Apple Biomater 2005;74: 570-81.
7. Xue L, Greisler HP. Biomaterials in the development and future of vascular grafts. J Vasc Surg 2003; 37:472-80
8. Sprague EA, Luo J, Palmaz JC. Human Aortic Endothelial Cell Migration onto Stent Surfaces under Static and Flow conditions. J Vasc Interv Radiol 1997;8(1Pt1):83-92.
9. Li S, Huang NF, Hsu S. Mechanotransduction in Endothelial Cell Migration. J Cell Biochem 2005;96:1110-26.
10. Chlen S, Li S, Shyy J.Y-J. Effects of Mechanical Forces on Signal

Transduction and Gene Expression in Endothelial Cells. Hypertension 1998;31:162-9.

11. Davies PF. Flow-mediated endothelial mechanotransduction. Physiol Rev 1995;75:519-60.
12. Page E, Cura M, Sprague E. Bare-Stent Technology and Its Utilization in the Treatment of Atherosclerotic Obstructive Disease. Vascular disease management 2010;7:95-102.
13. Langer R, Vacanti JP. Tissue engineering. Science 1993;260:920-6.
14. Asti A, Visai L, Dorati R, Conti B, Saino E, Sbarra S, et al. Improved cell growth by Bio-Oss/PLA scaffolds for use as a bone substitute. Technol Health Care. 2008;16:401-13.
15. Shimizu K, Ito A, Honda H. Enhanced Cell-Seeding into 3D Porous Scaffolds by Use of Magnetite Nanoparticles. J Biomed Mater Res B Appl Biomater 2006;77:265-72.
16. Lee JH, Lee SJ, Khang G, Leem HB. The Effect of Fluid Shear Stress on Endothelial Cell Adhesiveness to Polymer Surfaces with Wettability Gradient. Journal of Colloid and Interface Science 2000;230:84-90.
17. Li JP, Fu YN, Chen YR, Tan TH. J. JNK Pathway-associated phosphatase dephosphorylates focal adhesion kinase and suppresses cell migration. The journal of Biological Chemistry 2010;285(8):5472-8.
18. Xu W, Baribault H, Adamson ED. vinculin knockout results in heart and brain defects during embryonic development. Development 1998 ;125:327-37.
19. Zaidel-Bar R, Kam Z, Geiger B. Polarized downregulation of the paxillin-p130CAS-Rac1 pathway induced by shear flow. Journal of Cell Science 2005:118;3997-4007
20. Li S, Butler P, Wang Y, Hu Y, Han DC, Usami S et al. The role of the

dynamics of focal adhesion kinase in the mechanotaxis of endothelial cells. Proc Natl Acad Sci USA 2002; 99:3546-51.

21. Hu YL, Li S, Miao H, Tsou TC, Del Pozo MA, Chien S. Roles of microtubule dynamics and small GTPase Rac in endothelial cell migration and lamellipodium formation under flow. J Vasc Res 2002:39;465-76.
22. Ettenson DS, Gotlieb AI. Endothelial wounds with disruption in cell migration repair primarily by cell proliferation. Microvasc Res 1994;48:328-37.
23. Hsu PP, Li S, Li YS, Usami S, Ratcliffe A, Wang X, et al. Effects of Flow Patterns on Endothelial Cell Migration into a Zone of Mechanical Denudation. Biochem Biophys Res Commun 2001;285(3):751-9.
24. Albuquerque ML, Waters CM, Savla U, Schnaper HW, Flozak AS. Shear stress enhances human endothelial cell wound closure in vitro. Am J Physiol Heart Circ Physiol 2000;279:293-302.
25. Bednarz J, Thalmann-Goetsch A, Richard G, Engelmann K. Influence of vascular endothelial growth factor on bovine corneal endothelial cells in a wound-healing model. Ger J Ophthalmol 1996;5:127-31.
26. Zaidel-Bar R, Kam Z, Geiger B. Polarized downregulation of the paxillin-p130CAS-Rac1 pathway induced by shear flow. J Cell Sci 2005;118:3997-4007.
27. Wojciak-Stothard B, Ridley AJ. Shear stressinduced endothelial cell polarization is mediated by Rho and Rac but not Cdc42 or PI 3-kinases J Cell Biol 2003;161(2):429-39.
28. Li S, Chen BP, Azuma N, Hu YL, Wu SZ, Sumpio BE, et al. Distinct roles for the small GTPases Cdc42 and Rho in endothelial responses to shear stress. J Clin Invest 1999;103:1141-50.
29. Ridley AJ. Rho GTPases and cell migration. J. Cell Sci 2001;114:2713-22.
30. Kladakis SM, Nerem RM. Endothelial Cell Monolayer Formation: Effect

of Substrate and Fluid Shear Stress. Endothelium 2004;1:29-44.

31. Helmlinger G, Berk BC, Nerem RM. Pulsatile and steady flowinduced calcium oscillations in single cultured endothelial cells. J Vasc Res 1996;33**:**360-9.
32. Helmlinger G, Geiger RV, Schreck S, Nerem RM. Effects of pulsatile flow on cultured vascular endothelial cell morphology. J Biomech Eng 1991;113:123-31.
33. Malek A, Izumo S. Physiological fluid shear stress causes downregulation of endothelin-1 mRNA in bovine aortic endothelium. Am J Physiol 1992; 263:389-96.
34. Malek A, Izumo S. Mechanism of endothelial cell shape change and cytoskeletal remodeling in response to fluid shear stress. J Cell Sci 1996;109: 713-26.
35. Dull RO, Davies PF. Flow modulation of agonist (ATP)-response (Ca2+) coupling in vascular endothelial cells. Am J Physiol 1991;261:149-54.
36. Li S, Butler P, Wang Y, Hu Y, Han DC, Usami S, et al. The role of the dynamics of focal adhesion kinase in the mechanotaxis of endothelial cells. Proc. Natl. Acad Sci USA 2002;99:3546-51.
37. Holy CE, Shoichet MS, Davies JE. Engineering three-dimensional bone tissue in vitro using biodegradable scaffolds: Investigating initial cell-seeding density and culture period. J Biomed Mater Res 2000;51:376 -82.
38. Li Y, Ma T, Kniss DA, Lasky LC, Yang ST. Effects of filtration seeding on cell density, spatial distribution, and proliferation in nonwoven fibrous matrices. Biotechnol Prog 2001;17:935-44.
39. Vunjak-Novakovic G, Radisic M. Cell seeding of polymer scaffolds. Methods Mol Biol 2004;238:131-46.
40. Freed LE, Vunjak-Novakovic G, Biron R., Eagles D, Lesnoy D, Barlow S,

et al. Biodegradable polymer scaffolds for tissue engineering. Bio/ Technology 1994;12:689-93.

41. Freed LE, Marquis JC, Nohria A, Emmanual J, Mikos AG,Langer R. Neocartilage formation in vitro and in vivo using cells cultured on synthetic biodegradable polymers. J Biomed Mater Res. 1993;27:11-23

국문요약

인공혈관의 적절한 혈관 내피화를 위한 혈관 내피 세포의 이동 분석

<지도교수 박 종 철>

연세대학교 대학원 의과학과

강재경

혈관 우회술, 풍선 확장술, 스텐트 설치 시술 후에 일어나는 혈관 재협착의 대부분의 이유는 혈관 내피의 손상 때문이다. 혈관 내피 세포는 혈관의 가장 안 쪽을 이루고 있는 한 층의 편평한 세포이다. 손상된 혈관의 빠른 재혈관내피화는 혈전 현상이 생기는 것과 내막의 과다증식을 막아주는데 중요하다. 손상된 혈관은 초기에 혈관 내피세포의 이동을 시작으로 치유가 된다. 대부분의 혈관 내피 세포 이동에 관한 연구는 정적인 상태에서 진행이 되지만 신체 내에서 혈관 내피 세포는 계속해서 혈액의 흐름의 영향을 받고 있다. 혈액의 흐름에 의해 생기는 힘인 전단력은 세포의 모양 변화, 증식, 세포 골격의 재배치 등 많은 부분에 영향을 주는 것으로 알려져 있다.

이번 연구에서는 전단력이 가해진 상태에서 혈관 내피 세포의 이동을 평가하기 위해 Parallel plate chamber system를 설치 고안하였다. 창상 치유 모델 에서 세포 이동 방향과 배지의 흐름 방향이 같은 부분에서는 창상 부분 쪽으로 더 이동시키는 효과를 관

찰할 수 있었고 세포의 이동 방향과 배지의 흐름 방향이 반대인 부분에서는 전단력이 세포의 이동을 방해함을 알 수 있었다. 세포 각각의 움직임을 보기 위해 만든 모델에서는 전단력이 8 dyne/cm^2 일 때부터 세포가 전단력의 방향으로 움직이기 시작했다. 전단력을 8 dyne/cm^2을 가해 면역 염색법을 통해 Focal adhesion이 세포의 이동하는 앞 부분에 생긴다는 것과 세포 골격이 전단력의 방향으로 재배치 된다는 것을 관찰하였다. 이러한 결과를 바탕으로 전기 방사하여 얻은 지지체를 이용하여 지지체 내에 효과적으로 혈관 내피 세포의 균일하게 분포 하도록 Flow perfusion system을 이용하여 실험하였다. 세포가 부착된 지지체에 전단력을 가하면 지지체 위쪽에 있던 세포들이 효과적으로 지지체 내로 이동하는 것을 관찰하였다.

이 평가 방법은 혈액 내에서의 혈관 내피 세포 이동을 예측 가능하게 하고 그 결과를 바탕으로 스텐트나 인공 혈관 디자인에 도움을 줄 수 있을 것으로 예상된다.

핵심되는 말 : 혈관 내피 세포, 세포 이동, 전단력, 지지체, 기계적 주성